Preprints (www.preprints.org) | NOT PEER-REVIEWED | Posted: 16 February 2018 doi:10.20944/preprints201802.0107.v1

Peer-reviewed version available at Minerals 2018, 8, 155; doi:10.3390/min8040155

Article

Formation of Fe- and Mg-rich smectite under hyperalkaline conditions at Narra in Palawan, Philippines

Misato Shimbashi [1], Tsutomu Sato [2,*], Minoru Yamakawa [3], Naoki Fujii [3], Tsubasa Otake [2]

[1] Graduate School of Engineering, Hokkaido University N13W8, Kita-ku, Sapporo, Hokkaido 060-8628, Japan; shimbashi.m@gmail.com
[2] Division of Sustainable Resource Engineering, Faculty of Engineering, Hokkaido University, N13W8, Kita-ku, Sapporo, Hokkaido 060-8628, Japan; tomsato@hokudai.ac.jp
[3] Radioactive Waste Management Funding and Research Center, Akashi-cho 6-4, Chuo-ku, Tokyo 104-0052, Japan; fujii@rwmc.or.jp
* Correspondence: tomsato@hokudai.ac.jp; Tel.: +81-11-706-6305

Academic Editor: name
Received: date; Accepted: date; Published: date

Abstract: Formation of Fe- and Mg-rich smectite and zeolite under alkaline conditions is concerned as secondary minerals after alkaline alteration of bentonite in a repository of radioactive wastes. It might be crucial for safety assessment whether smectite will be formed or not as secondary minerals after alkaline alteration of bentonite. In present paper, Fe- and Mg-rich smectite which are currently interacting with hyperalkaline groundwater was found at Narra in Palawan, Philippines. Mineralogical and geochemical investigation was conducted to understand formation process of smectite and factors determined secondary mineral species. Our study revealed a certain amount of smectite may have been produced under hyperalkaline conditions, altered from amorphous or poorly crystalline material such as M-S-H and F-S-H. Key factor which decides smectite or zeolite as secondary minerals after alkaline alteration of bentonite might be whether nuclei of M-S-H and/or F-S-H will be formed or not. This might be decided by the presence of dissolved Mg^{2+} and Fe^{2+} in the system. Our suggested formation process of smectite under alkaline conditions is analogue with generally-accepted model of smectite formation that might have been occurred on early Mars.

Keywords: Fe- and Mg-rich smectite; alkaline; ophiolite; M-S-H; F-S-H; C-S-H; geological disposal; natural analogue; Mars

1. Introduction

Smectite is ubiquitous clay mineral in diverse surface or near-surface environment on the Earth and has used in many industrial fields. For example, bentonite, which mainly consists of montmorillonite in smectite group, is planned to be used as buffer materials for geological disposal of radioactive wastes due to its favorable properties of smectite such as low permeability and high cation exchange capacity. However, loss of barrier function of bentonite has been concerned by reactions with hyperalkaline leachates from cementitious materials in the repository. Many laboratory experiments have been conducted to understand geochemical reactions of bentonite under hyperalkaline conditions for the safety assessment. Among those, many previous studies used NaOH, $Ca(OH)_2$ and/or KOH solution as the hyperalkaline leachates, and reported the formation of zeolite [1–3]. However, there is a significant disparity in time scales and complexity of reaction fields between laboratory experiments and actual disposal environments. Therefore,

© 2018 by the author(s). Distributed under a Creative Commons CC BY license.

Preprints (www.preprints.org) | NOT PEER-REVIEWED | Posted: 16 February 2018 doi:10.20944/preprints201802.0107.v1

Peer-reviewed version available at Minerals 2018, 8, 155; doi:10.3390/min8040155

"natural analogue studies" are unambiguously necessary to bridge such a gap for long-term safety assessment and not only expert's but also public acceptances.

A previous natural analogue study examined interactions between bentonite and natural alkaline fluids at Zambales ophiolite in Luzon, Philippines [4]. They reported that bentonite alteration zone was limited within 5 mm because of clogging at the interface by secondary formed minerals such as goethite, K-feldspar and Fe- and Mg-rich smectite. They attributed the limited alteration of bentonite at the interface to this clogging. Because smectite has properties such as low permeability and high cation exchange capacity as mentioned above, the formation of smectite at the interface might play an important role for hydrologic barrier and nuclides isolation performance. Therefore, smectite formation and subsequent clogging after dissolution of bentonite in the repository would contribute to maintain a required barrier performance of bentonite. This geochemical reaction presumably occurs in the repository because Fe might be supplied from other engineered barrier components such as over pack and prefabricated engineering barrier, and Mg might be derived from bentonite itself and groundwater. Therefore, the natural analogue study at Zambales ophiolite showed important implication for understanding of long-term bentonite-hyperalkaline interaction. However, that interaction between bentonite and alkaline fluids has already finished so that fluid chemistry for the formation at that site was poorly understood. Therefore, formation process of smectite and factors determined secondary mineral species are still uncertain. For this reason, it is not enough to conclude the possibility of smectite formation after bentonite dissolution in the repository from the results of natural analogue study at Zambales ophiolite.

In Philippines, there are many hyperalkaline springs from present-day serpentinization of ultramafic rock. The authors found Fe- and Mg-rich smectite in underground sediments at Narra in Palawan, Philippines and hyperalkaline fluids at the same site. In this site, study on stability of smectite or formation of smectite under hyperalkaline conditions was available, although there is unfortunately no bentonite. Therefore, in this study, mineralogical and geochemical investigation was conducted to understand geochemical reaction of smectite under hyperalkaline condition.

2. Geological setting and samples

The Philippines Archipelago is surrounded by some major plates such as Eurasian Plate, Pacific Plate and Indo-Australian Plate. Palawan is one of the islands situated on the south-eastern margin of the South China Sea. Geology in the south and central Palawan is dominated by Palawan ophiolite. Palawan ophiolite was detached from underlying upper mantle following initiation of subduction at a spreading ridge in the Palaeocene, and thrust onto the Asian margin during collision which began in the late Eocene [5]. The emplacement of the ophiolite was taken place between Late Oligocene and Early Miocene [6]. The stratigraphic sequence in ophiolite is from tectonized peridotites, cumulate peridotites, layered gabbro, sheeted dike complex, pillow basalts and pelagic sedimentary rocks. In the ophiolite observed at the surface of ground, the peridotites have commonly changed into serpentinite. This occurs in the mantle wedge at depths of 30 to 40 km below the surface, which is called as "(high temperature) serpentinization".

Samples were collected at Narra in the central Palawan. Figure 1 shows sampling sites and the studied area on a bird's-eye photo. The main sampling site (Narra3-2) is alluvial fan channel distributed on a gentle slope of Palawan ophiolite basement. The basement is composed of partially serpentinized harzburgite and small amount of gabbro (Figure 1). Spring water spouts along fractures of Palawan ophiolite on the top of the fan channel (Narra3-1), and flowing to Narra3-2 on the surface fan deposition as surface waters. Surface of Narra3-2 is covered by calcite travertine. Trench and drilling excavations were conducted at Narra3-2. Figure 2 shows bird's-eye photo and cross-sectional view of the main sampling site (Narra3-2). Below the travertine deposit, clastic sediments originated from Palawan ophiolite were deposited.

Preprints (www.preprints.org) | NOT PEER-REVIEWED | Posted: 16 February 2018 doi:10.20944/preprints201802.0107.v1

Peer-reviewed version available at Minerals 2018, 8, 155; doi:10.3390/min8040155

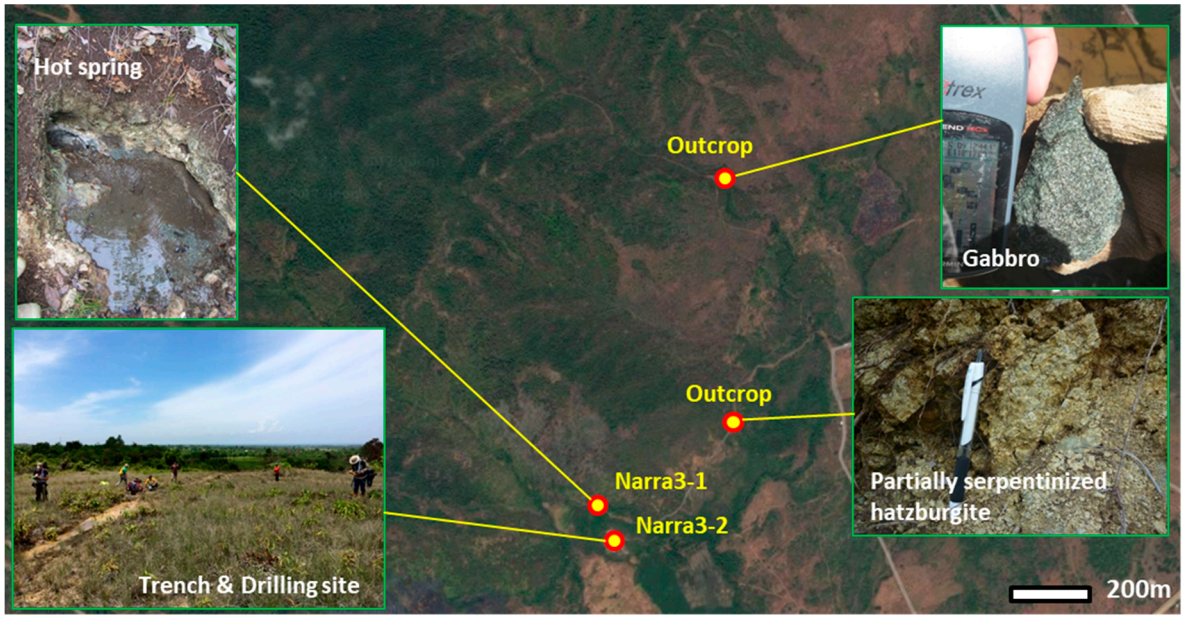

Figure 1. Bird's-eye photo and sampling sites of the studied area

Locations of trenches and drill holes are shown in Figure 2(a). Solid samples were collected from each trenches and drill holes. Because the clastic sediments could be collected spatially larger than basement, 20 samples collected from all over the clastic sediments layer were mainly provided to detailed analysis. Among those, core samples from the deepest drill hole (DH4) were analyzed in more detail to understand long-term interaction between clastic sediments and groundwater. Wooden branches in clastic sediments at different depth are collected from Trench5 (T5) to estimate time from their deposits. Location of core samples from DH4 and wooden branches from T5 were shown in cross-sectional view of Narra3-2 (Figure 2(b)).

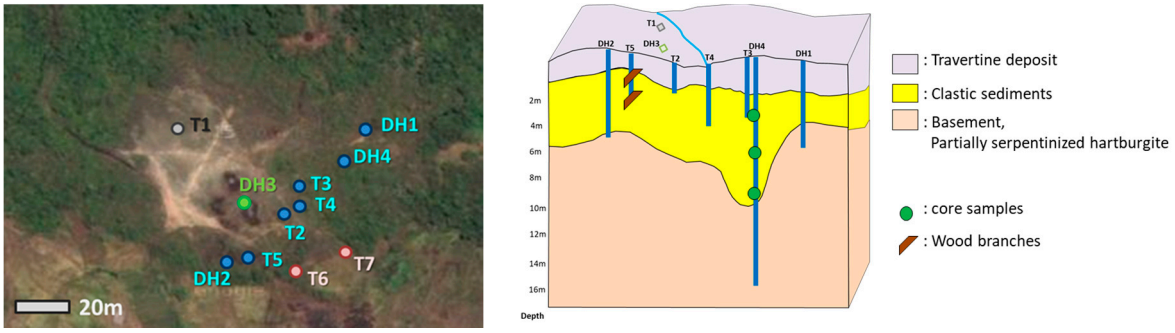

(**a**) (**b**)

Figure 2. (**a**) Bird's-eye photo of Narra3-2 ; (**b**) cross-sectional view of Narra3-2

Water samples were collected from groundwater discharged from the trench walls and drill holes (T1-7 and DH1-4), surface water from different locations at Narra3-2 (upper stream, middle stream and lower stream) as well as spring water at Narra3-1.

3. Methods

To obtain data on chemistry of water samples, the following analyses were conducted. Temperature, pH and ORP were measured at the site. Alkalinity was measured by titrating HNO_3 into 50 mL of water samples that had been filtered through 0.45 μm polytetrafluoroethylene (PTFE) membrane filters at the site. Additional filtered water samples were obtained by filtering through 0.2 μm PTFE membranes for analyses of cations and anions. Concentration of major cations was analyzed by atomic adsorption spectrometry (ZA3300, Hitachi, Co. Ltd.), except concentration of Al

Preprints (www.preprints.org) | NOT PEER-REVIEWED | Posted: 16 February 2018 doi:10.20944/preprints201802.0107.v1

Peer-reviewed version available at Minerals 2018, 8, 155; doi:10.3390/min8040155

was analyzed by atomic adsorption spectrometry (Z-5010, Hitachi, Co. Ltd.), and concentration of Si was analyzed by Spectrophotometry (U-1100, Hitachi, Co. Ltd.). Concentration of major anions was analyzed by ion chromatography (ICS-2100, Thermo, Co. Ltd.).

Clastic sediments and rock samples were air-dried or freeze-dried, and then conducted X-ray diffraction analysis to determine the mineralogical compositions by using an X-ray diffractometer (Multiflex, Rigaku, Co. Ltd.) equipped for graphite-monochromatic CuKα radiation and operated at 40 kV and 40 mA. The randomly oriented powder samples were scanned from 5°to 70°in 2θ at scanning speed of 0.01°/s. Samples were separated in fraction less than 2 μm from course fraction by ultrasonic dispersion and centrifugation. Preferred orientation specimens were prepared by drying <2 μm diameter fraction suspension and mounting on glass slides at room temperature with and without ethylene glycol solvation. Ethylene glycol solvation was conducted with ethylene glycol vapor at 60°C for more than 12 hours. They were analyzed by using an X-ray diffractometer (RINT1200, Rigaku, Co. Ltd.) equipped for CuKα radiation at 30 kV and 20 mA. The samples were scanned from 2°to 40°in 2θ at scanning speed of 0.02°/s. The randomly oriented powder samples of <2 μm diameter fraction were measured to observe 060 reflection of clay minerals. 06l reflection is useful to distinguish dioctahedral and trioctahedral clay minerals because d060 is sensitive to the degree of occupancy and the size of cations in octahedral sheets. The samples were scanned from 59°to 63° in 2θ by a fixed time scan method with 10 seconds for each 0.02 degree.

Selected core samples were embedded into a resin to make thin sections. Occurrences of infilling materials at matrix of clastic sediments were observed and quantitative analysis of their chemical compositions was conducted by using an Electron Probe Micro Analyzer (JXA-8530F, JEOL, Co. Ltd.). Structural formula of smectite was determined by following procedures: (1) assign all Si^{4+} to the tetrahedral site, (2) assign all Al^{3+} to the tetrahedral site until tetrahedral site occupancy is 4, and then assign Al^{3+} to the octahedral site, (3) assign all Fe to the tetrahedral site until tetrahedral site occupancy is 4 under assumption that Fe is present as Fe^{3+}, and then assign Fe to the octahedral site (4) assign all Mg^{2+} to the octahedral site, (5) assign all Ca^{2+}, Na^{+} and K^{+} to the interlayer site.

Minerals at matrix observed in thin sections were picked up by using micromanipulator (Quick Pro, Micro Support Co. Ltd.) and hard tool probe (CP-005, Micro Support Co. Ltd.). They were analyzed by Transmission Electron Microscope (JEM-2010, JEOL, Co. Ltd.) for characterization of minerals at matrix. Energy Dispersive X-ray Spectroscopy equipped with TEM was also used to confirm that target particles were picked up.

Radioactive carbon (^{14}C) dating of wooden branches in the clastic sediments was conducted by using tandem-type accelerator mass spectrometer (15SDH-2, National Electrostatics Corporation). ^{14}C decay with time, and its half-life is 5730 years. Therefore, ^{14}C dating is suitable for estimation of time shorter than tens thousands of years. When wood is alive, containing carbon isotope is similar with that of atmosphere. However, ^{14}C is just decreasing in wooden branches after stopping biological activity. Therefore, ^{14}C in samples yielded burial age of wooden branches. Preprocessing procedure of graphitization of samples was done at Toki Research Institute of Isotope Geology and Geochronology.

"The Geochemist's Workbench" software package was used to carry out the thermodynamic calculation to obtain phase diagrams for Mg-Si-Al-Na system. In the calculation, thermodynamic database "thermoddem" provided by BRGM was used after incorporation of equilibrium constants for magnesium silicate hydrate (M-S-H) reported in a previous study [7].

4. Results

4.1. Fluids analyses

On-site measurements and concentrations of major cations and anions are reported in Table 1. Results of the chemical analyses show that both spring water at Narra3-1 and groundwater at Narra 3-2 were hyperalkaine (pH> 11; Table 1), and have very similar geochemical characteristics in the stiff diagrams (Figure 3). They have same characteristics such as low dissolved Mg, Si, Fe, HCO_3

Preprints (www.preprints.org) | NOT PEER-REVIEWED | Posted: 16 February 2018 doi:10.20944/preprints201802.0107.v1

Peer-reviewed version available at Minerals 2018, 8, 155; doi:10.3390/min8040155

concentrations and high dissolved Ca concentration regardless of the different sampling depths (~11m to 1m below the surface) for the groundwater. This chemistry of those samples is similar with that of groundwater from other representative ophiolites [8–11], and similar with leachates from cement degradation.

Table 1. On-site measurements and concentrations of major cations and anions in ppm

Sample	T [℃]	pH	ORP [mV]	Na^{+}	K^{+}	Mg^{2+}	$Fe^{(2+3)+}$	Al^{3+}	Ca^{2+}	Si^{2+}	Cl^{-}	SO_4^{2-}	HCO_3^{-}
Narra 3-1	38.6	11.16	-450	48.6	2.94	0.02	0.02	0.07	37.5	0.9	29.5	0.18	0.09
T1	30.3	11.31	-176 [1]	44.6	2.12	0.02	0.02	0.01	32.2	0.7	25.6	0.08	0.77
DH2	35.9	11.18	-113	40.3	2.66	0.03	0.03	0.03	24.8	5	31.3	0.10	5.6
T5	29.9	11.36	-152	48.2	2.24	<0.01	0.01	0.13	44.8	4.1	27.8	<0.01	3.6
T6	27.2	10.96	-107	50.1	2.46	0.01	0.02	0.19	24.6	5.77	28.5	1.92	9.2
DH3	33.5	11.29	-99	51.2	2.72	0.01	0.02	0.07	33.9	2.8	28.7	0.12	1.2
T2	28.8	11.39	-160	46.1	2.32	0.02	0.02	0.08	26.9	2.5	27.3	0.13	0.67
T7	27.7	11.16	-141	49.1	2.02	<0.01	0.02	0.18	26.8	4.27	28.6	0.63	8.9
T4	33.4	11.17	-30	47.1	2.54	0.02	0.03	0.10	36.4	2.3	28.5	0.21	2.1
T3	33.7	11.37	-111	50.4	2.39	0.01	0.05	0.08	48.5	2.5	27.0	0.02	<0.01
DH4	33.0	11.39	-119	51.8	2.96	0.02	0.03	0.06	22.4	2.9	21.1	0.14	2.8
DH1	30.9	11.08	-79	51.1	3.56	<0.01	0.04	0.07	10.4	8	31.6	0.83	2.3
Upper stream	32.5	9.3	120	52.6	2.55	18.0	0.02	<0.01	27.3	11	36.6	0.58	275.5
Middle stream	33.2	9.64	120	52.4	2.55	16.0	0.02	<0.01	22.9	10	36.2	0.53	105.9
Lower stream	32.4	9.73	115	51.7	2.42	5.00	0.02	<0.01	9.2	4.2	35.3	0.34	100.4

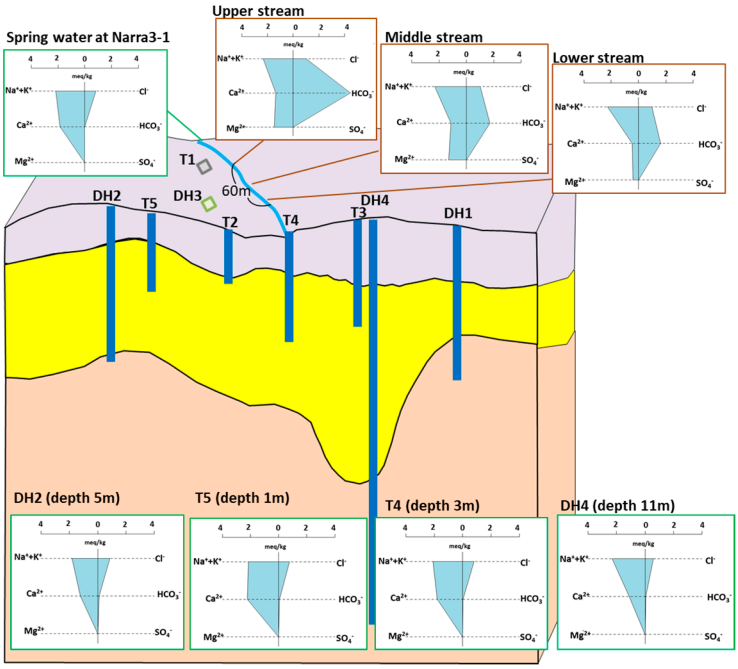

Preprints (www.preprints.org) | NOT PEER-REVIEWED | Posted: 16 February 2018 doi:10.20944/preprints201802.0107.v1

Peer-reviewed version available at Minerals 2018, 8, 155; doi:10.3390/min8040155

Figure 3. Stiff diagrams of representative water samples (spring water at Narra3-1, surface water at Narra3-2, groundwater at Narra3-2 collected from DH2, T5, T4 and DH4)

On the other hand, surface water has different characteristics from those of hyperalkaline groundwater (Figure 3). Surface water are less alkaline (pH<10), and showed higher Mg^{2+} and HCO_3^- concentrations than those in the hyperalkaline groundwater and spring water (Figure 3). Moreover, dissolved Ca, Mg and HCO_3 concentrations decreased from the upper stream to the lower stream (Figure 3).

4.2. XRD analyses

Smectite was identified in all the clastic sediment samples after XRD measurements of ethylene glycol-solvated and preferred orientation samples. Although smectite was found to be present under hyperalkaline conditions, it is still uncertain whether smectite at this site was produced under this condition or transported from other places because of sediments. Detail analyses were conducted to understand formation process of smectite.

Figure 4 shows XRD patterns of the samples collected from DH4 (3-10m in depth). They were collected from clastic sediments layer. Smectite, serpentine and amphibole were detected in those samples. Besides, tobermorite, pyroxene and calcite were detected in some of them (Figure 4).

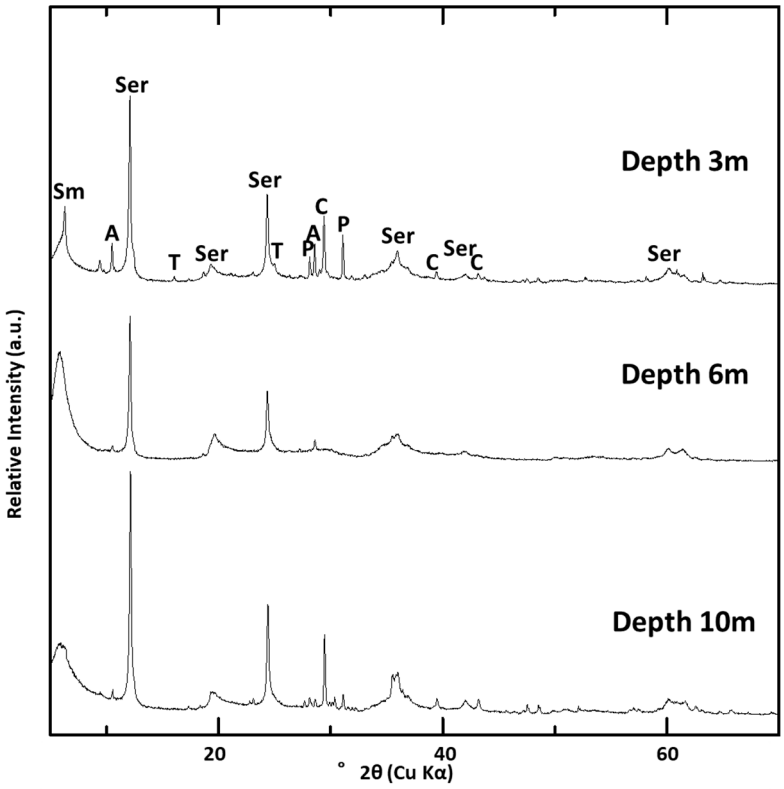

Figure 4. XRD spectra of randomly oriented powder samples of DH4 at each depth (3m, 6m and 10m) Sm: smectite; Ser: serpentine; T: tobermorite; P: pyroxene; A: amphibole; C: calcite

T1 (3m in depth) is located upper part of alluvial fan channel than other trenches and drill holes (Figure 2). From XRD analysis of samples collected from T1, only calcite was detected. Compared to depth of travertine deposits for each trenches and drill holes, travertine deposits were thick at upper part of alluvial fan channel, which is T1, than other trenches and drill holes.

Figure 5 shows preferred orientation XRD spectra and 060 reflection of <2 μm fraction. The intensity of peak assigned to smectite is higher in samples from deeper parts of DH4 (6m and 10m in depth) compared to that from shallower parts of DH4 (3m in depth). This trend was also observed for most of samples collected from clastic sediments layer at each trenches and drill holes.

Preprints (www.preprints.org) | NOT PEER-REVIEWED | Posted: 16 February 2018 doi:10.20944/preprints201802.0107.v1

Peer-reviewed version available at Minerals 2018, 8, 155; doi:10.3390/min8040155

From its 060 reflection, smectite is identified as nontronite because of the position of 060 reflection in smectite-rich samples (e.g. Figure 5(e)(f)).

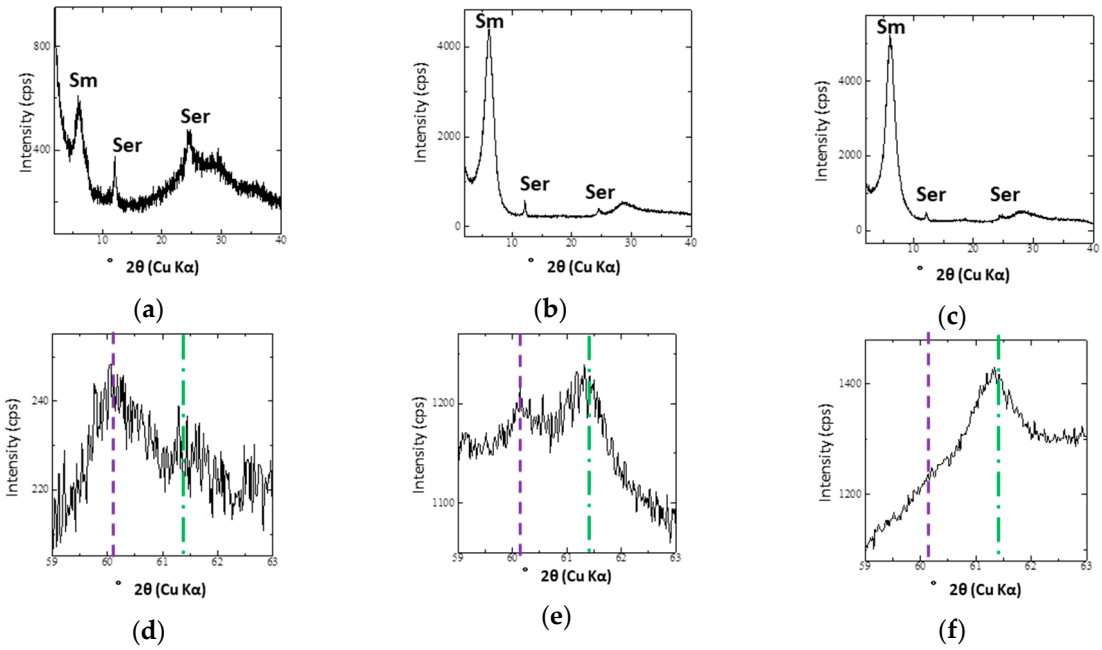

Figure 5. XRD spectra of <2μm fraction of DH4 at each depth : (**a**) Oriented XRD spectra at depth 3m ; (b) Oriented XRD spectra at depth 6m ; (c) Oriented XRD spectra at depth 10m ; (d) XRD spectra of 060 reflection at depth 3m ; (e) XRD spectra of 060 reflection at depth 6m ; (f) XRD spectra of 060 reflection at depth 10m ; Sm: smectite; Ser: serpentine

4.3. EPMA analyses

Occurrences of infilling materials at matrix of clastic sediments collected from DH4 (3m and 6m in depth) were observed by EPMA (Figure 6). Those samples were chosen for detailed analysis because smectite content is different (Figure 5(a)(b)). Minerals at matrix could be divided mainly into 2 categories. One is solid phase with Si, Fe and Mg, and the other is solid phase with Si and Ca. The solid phase with Si, Fe and Mg was present as major minerals that filled matrix of clastic sediments.

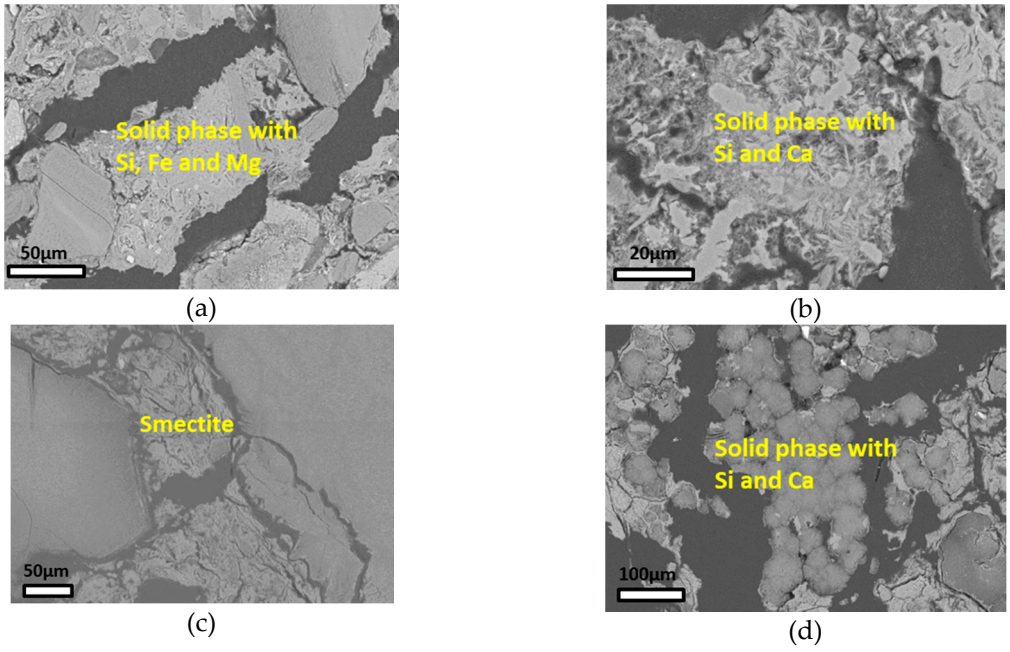

Preprints (www.preprints.org) | NOT PEER-REVIEWED | Posted: 16 February 2018 doi:10.20944/preprints201802.0107.v1

Peer-reviewed version available at Minerals 2018, 8, 155; doi:10.3390/min8040155

Figure 6. Occurrences of minerals that filled matrix of clastic sediments from DH4 at each depth : (**a**) solid phase with Si, Fe and Mg at depth 3m. ; (**b**) solid phase with Si and Ca at depth 3m. ; (c) Smectite at depth 6m. ; (d) solid phase with Si and Ca at depth 6m.

From chemical compositions determined by EPMA, most of minerals at matrix at depth 6m were assigned as smectite. However, solid phase with Si, Fe and Mg at matrix at depth 3m was not assigned as smectite for the following reasons. Chemical compositions of smectite at depth 6m and minerals that filled matrix at depth 3m are similar except that Si content of minerals that filled matrix at depth 3m is lesser than that of smectite. Crystal structure of phyllosilicates is classified in 2 layer types, 1:1 layers and 2:1 layers. Smectite has 2:1 layers in which one octahedral sheet is sandwiched between two tetrahedral sheets, and some clay minerals such as serpentine has 1:1 layers in which one octahedral sheet is bonded to one tetrahedral sheet. Fe- and Mg-rich smectite have Mg, Fe as major cations in octahedral sheets with small amount of isomorphous substitution of Al. And it has Si as major cations in tetrahedral sheets with small amount of isomorphous substitution of Al and Fe^{3+}. Therefore, (Fe+Mg)/Si ratio will indicate layer types. Table 2 shows (Fe+Mg)/Si ratio of ideal smectite, ideal serpentine, smectite at depth 6m and minerals at matrix at depth 3m. (Fe+Mg)/Si ratio of ideal smectite is about 0.5-0.8, and (Fe+Mg)/Si ratio of ideal serpentine is about 1.5. (Fe+Mg)/Si ratio of minerals at matrix at depth 3m is about 1.24-1.51, while that at depth 6m, which is assigned to smectite, is about 0.55-0.88. This indicates that minerals at matrix at depth 3m might not form 2:1 layers, and were not assigned as smectite. This phase was characterized in section 4.4 by using TEM.

Table 2. (Fe+Mg)/Si ratio of ideal smectite, ideal serpentine, smectite from DH4 at depth 6m and minerals at matrix of clastic sediments from DH4 at depth 3m. N represents number of analyzed points.

	Ideal smectite	Ideal serpentine	Smectite at depth 6m	Minerals at matrix at depth 3m
(Fe+Mg)/Si	0.5-0.8	1.5	0.55-0.88	1.24-1.51
Analyzed points	-	-	14	16

Solid phase with Si and Ca was partially observed at matrix of clastic sediments (Figure 6). Chemical contents of this mineral are mainly Si, Ca. Ca/Si ratio at each points is about 0.4-0.8. They contain small amount of Fe.

4.4. TEM observations

Solid phase with Si, Fe and Mg that filled matrix of clastic sediments from DH4 at depth 3m was not identified as smectite (see section 4.3). They were picked up by using micromanipulator for TEM observation, and confirmed that target particles were surely picked up by chemical analysis of constituent using EDS equipped with TEM. Figure 7 shows TEM image, and the corresponding selected-area diffraction (SAD) pattern. These particles formed indeterminate aggregate (Figure 7(a)). SAD pattern shows 3 diffuse rings (Figure 7(b)). The observed d-spacing is 4.55 Å, 2.59 Å and 1.53 Å. Previous study reported that M-S-H is low crystalline phase with broad humps at 4.51 Å, 3.34 Å, 2.56 Å and 1.54 Å by XRD [7], and those d-spacings, except for 3.34 Å, are very similar with observed d-spacing of particle picked up from matrix of clastic sediments from DH4 at depth 3m.

Preprints (www.preprints.org) | NOT PEER-REVIEWED | Posted: 16 February 2018 doi:10.20944/preprints201802.0107.v1

Peer-reviewed version available at Minerals 2018, 8, 155; doi:10.3390/min8040155

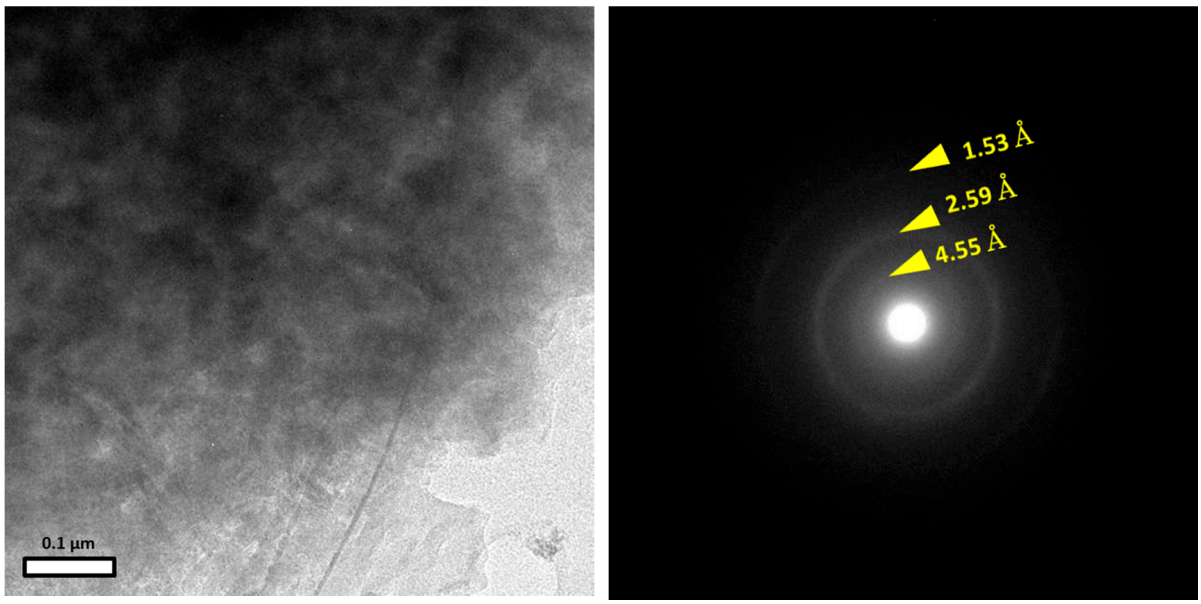

(**a**) (**b**)

Figure 7. TEM results for solid phase with Si, Fe and Mg at matrix of clastic sediments from DH4 at depth 3m: (**a**) Low magnified image. ; (**b**) SAD pattern of the area in (a).

4.5. ^{14}C dating

^{14}C dating of wooden branches in the clastic sediments collected from T5 at different depth yields 2443±46 years and 1209±46 years. ^{14}C dating of wooden branches in sediments collected from different depth at T5 shows burial age of wooden branches from deeper parts is older than that from shallower parts.

Preprints (www.preprints.org) | NOT PEER-REVIEWED | Posted: 16 February 2018 doi:10.20944/preprints201802.0107.v1

Peer-reviewed version available at Minerals 2018, 8, 155; doi:10.3390/min8040155

5. Discussion

5.1. Origin of hyperalkaline groundwater and its relation to alkaline surface water

Hyperalkaline groundwater at Narra3-2 and spring water at Narra3-1 have same characteristics (Figure 3). This chemistry of those samples is similar with that of groundwater from other representative ophiolites [8–11]. They have indicated that the geochemical characteristics of those fluids are governed by geochemical reactions of meteoric waters with ultramafic rocks [10]. Therefore, chemistry of both groundwater and spring water at the site are also likely caused by geochemical reactions of meteoric water with Palawan ophiolite.

On the other hand, alkaline surface water at Narra3-2 showed higher Mg^{2+} and HCO_3^- concentrations than those in the hyperalkaline groundwater and spring water (Figure 3) although the field observation suggests that part of the surface water is possibly derived from the spring water. This may be due to mixing of the spring water with other surface water that are enriched in Mg and HCO_3, which was derived from weathering of ultramafic rocks with meteoric waters [10]. Moreover, dissolved Ca, Mg and HCO_3 concentrations decreased from upper stream to lower stream. This is probably due to precipitation of carbonate minerals. The carbonate minerals may precipitate when the spring water become oversaturated in term of carbonate minerals by the mixing with other surface water that contain Mg^{2+} and HCO_3^- at near neutral pH. This is consistent with that travertine deposits were thicker at upper part of alluvial fan channel (T1) than that at other trenches and drill holes. Clastic sediments were covered by travertine deposit. Consequently, spring water spouts at Narra3-1, and formed travertine deposit at Narra3-2 after deposition of clastic sediments at the site. Because surface water at Narra3-2 has different types from hyperalkaline groundwater (Figure 3), mixing of hyperalkaline groundwater at Narra3-2 and surface water in subsurface environment was not occurred currently at least.

5.2. Evidence of the interaction between clastic sediments and hyperalkaline groundwater

Solid phases with Si and Ca were formed at matrix of clastic sediments from DH4 (3m and 6m in depth) (Figure 6(b)(d)). Among minerals that detected in XRD analysis, mineral with Si and Ca is tobermorite. Therefore, the solid phases with Si and Ca at matrix of clastic sediments would be tobermorite. Previous study reported formation of 14Å tobermorite-like C-S-H at room temperature [12]. C-S-H has well known to form under alkaline pH such in concrete matrix [13]. Therefore, C-S-H formation under alkaline conditions primary formed as infilling materials at matrix of clastic sediments and precursor of the observed tobermorite. The presence of authigenic tobermorite consequently indicates that the infilling materials at matrix of clastic sediments formed by direct precipitation from hyperalkaline groundwater and/or interaction between the clastic sediments and hyperalkaline groundwater. In situ geochemical reaction involved with hyperalkaline groundwater would also be supported by the evidence of discharge of hyperalkaline groundwater from trench walls and drill holes.

5.3. Identification of the solid phase with Si, Fe and Mg

In the clastic sediments, from the results of XRD and EPMA, smectite was also observed as infilling materials (Figure 6(c)). In general, smectite is group name for expandable clay minerals and chemically divided into two sub groups such as dioctahedral smectite and trioctahedral smectite. The sub groups are mainly classified by valence of cations in octahedral sheets. Major cations in octahedral sheets of smectite are mainly Al^{3+} or Fe^{3+} for dioctahedral smectite and Mg^{2+} or Fe^{2+} for trioctahedral smectite. The smectite observed in the sediments was identified as nontronite based on 060 reflection in XRD patterns (Figure 5). Nontronite ordinary consists Fe^{3+} as main cations in octahedral sheets, and it is classified as dioctahedral smectite. Therefore, Fe in smectite might be mainly ferric state. However, smectite that filled matrix of clastic sediments from DH4 at depth 6m has Mg^{2+} with wide range of Fe/Mg ratio from 1.1 to 2.9, which is different from ideal nontronite.

Preprints (www.preprints.org) | NOT PEER-REVIEWED | Posted: 16 February 2018 doi:10.20944/preprints201802.0107.v1

Peer-reviewed version available at Minerals 2018, 8, 155; doi:10.3390/min8040155

Chemical composition of smectite from DH4 at depth 6m is between nontronite and trioctahedral smectite. This type of smectite is previously reported [14,15]

On the other hand, solid phase with Si, Fe and Mg at matrix of clastic sediments from DH4 at depth 3m was not identified as smectite (see section 4.3). This is consistent with the result of preferred orientation XRD analysis that shows smectite is poor in samples from DH4 at depth 3m compared to those at deeper depth (Figure 5 (a)(b)(c)). Major infilling materials would be separated in fraction less than 2 µm from course fraction by ultrasonic dispersion and centrifugation, and only smectite and serpentine were detected from XRD pattern of the fraction less than 2 µm (Figure 5(a)). Therefore, solid phase with Si, Fe and Mg at matrix of clastic sediments from DH4 at depth 3m would be considered to be serpentine as shown in the XRD pattern or X-ray amorphous material. The d-spacing obtained from SAD pattern of particle picked up from matrix of clastic sediments from DH4 at depth 3m are very similar with that of M-S-H reported previously [7]. M-S-H might be precursor of phyllosilicates such as smectite, talc, serpentine and sepiolite [7,16,17], although this is still controversial. In terms of Fe, previous study reported nuclei of a trioctahedral ferrous stevensite under reducing condition by aging coprecipitated gel of silica and Fe^{2+}-sulphate at low temperature (75 °C) [18]. In this laboratory experiment, although crystallization of the nuclei into smectite was not observed under reducing condition in 15 days, subsequent oxidation induced rapid crystallization of ferric nontronite-like smectite for a few weeks. This synthetic smectite has broad peaks with d-spacing at 14-15.5 Å, 4.54 Å, 3.41 Å, 2.61 Å, 2.28 Å, 1.70Å and 1.52 Å in the XRD pattern. Similar d-spacing was observed by evolution of Fe^{3+}-Si coprecipitates at 100 °C and 150 °C [19], and reported d-spacing at 4.45 Å, 2.56 Å, 1.71 Å, 1.51 Å and 1.29 Å by TEM. Table 3 shows d-spacing of solid phase with Si, Fe and Mg at matrix from DH4 at depth 3m, M-S-H [7], Fe^{2+}- Si coprecipitates [18], and Fe^{3+}-Si coprecipitates [19]. From this data shown in Table 3, solid phase with Si, Fe and Mg that infilled matrix of clastic sediments from DH4 at depth 3m have similar structure with not only M-S-H [7], but also Fe^{2+}- Si coprecipitates [18], and Fe^{3+}-Si coprecipitates [19]. Therefore, solid phase with Si, Fe and Mg as infilling materials from shallower parts might be amorphous or poorly crystalline material related to M-S-H and F-S-H.

Table 3. Comparison of d-spacing of solid phase with Si, Fe and Mg at matrix from DH4 at depth 3m measured by TEM, M-S-H measured by XRD [7], Fe^{2+}-Si coprecipitates measured by XRD [18], and Fe^{3+}-Si coprecipitates measured by TEM [19]. All d-spacing in Å.

Minerals at matrix from DH4 at depth 3m	M-S-H	Fe^{2+}-Si coprecipitates	Fe^{3+}-Si coprecipitates
-	-	14-15.5	-
4.55	4.51	4.54	4.45
-	3.34	3.41	-
2.59	2.56	2.61	2.56
-	-	2.28	-
-	-	1.70	1.71
1.53	1.54	1.52	1.51
-	-	-	1.29

5.4. Formation of Fe- and Mg-rich smectite under hyperalkaline conditions

Smectite was observed as infilling materials at matrix of clastic sediments as well as tobermorite (Figure 6). This might indicate smectite might be also formed under alkaline conditions. However, smectite is known to be produced by weathering of ultramafic minerals such as olivine and pyroxene under non-alkaline conditions. This remains uncertainties whether smectite at this

Preprints (www.preprints.org) | NOT PEER-REVIEWED | Posted: 16 February 2018 doi:10.20944/preprints201802.0107.v1

Peer-reviewed version available at Minerals 2018, 8, 155; doi:10.3390/min8040155

site was produced under this condition or transported from other places. It is very important to determine origin of the smectite. If the smectite formed under hyperalkaline condition at the site, this study will focus on smectite formation under hyperalkaline condition. On the contrary, if the smectite formed, transported and deposit at the site, this study will focus on smectite stability under hyperalkaline condition.

Smectite is rich in clastic sediments from deeper parts, and smectite was formed as infilling material at matrix of clastic sediments (e.g. sample from DH4 at depth 6m, Figure 6(c)). On the other hand, amorphous or poorly crystalline material such as M-S-H and F-S-H was formed as infilling material at matrix of clastic sediments from shallower parts (e.g. sample from DH4 at depth 3m, see section 5.3). Figure 8 shows a phase diagram for Mg-Si-Al-Na system. Chemical compositions of hyperalkaline groundwater are plotted within the stability fields of smectite (saponite) and serpentine (chrysotile). However, those fluids are not plotted in boundary of serpentine and smectite. When those thermodynamically stable phases are suppressed, they are plotted along the solubility line of M-S-H. This indicates concentrations of dissolved Mg and Si in the hyperalkaline groundwater are controlled by dissolution or precipitation of M-S-H, and not by dissolution or precipitation of stable phase such as serpentine and smectite. As mentioned above, from EPMA and TEM observations, M-S-H formed at matrix of clastic sediment. As consequence, M-S-H would be precipitated from hyperalkaline groundwater.

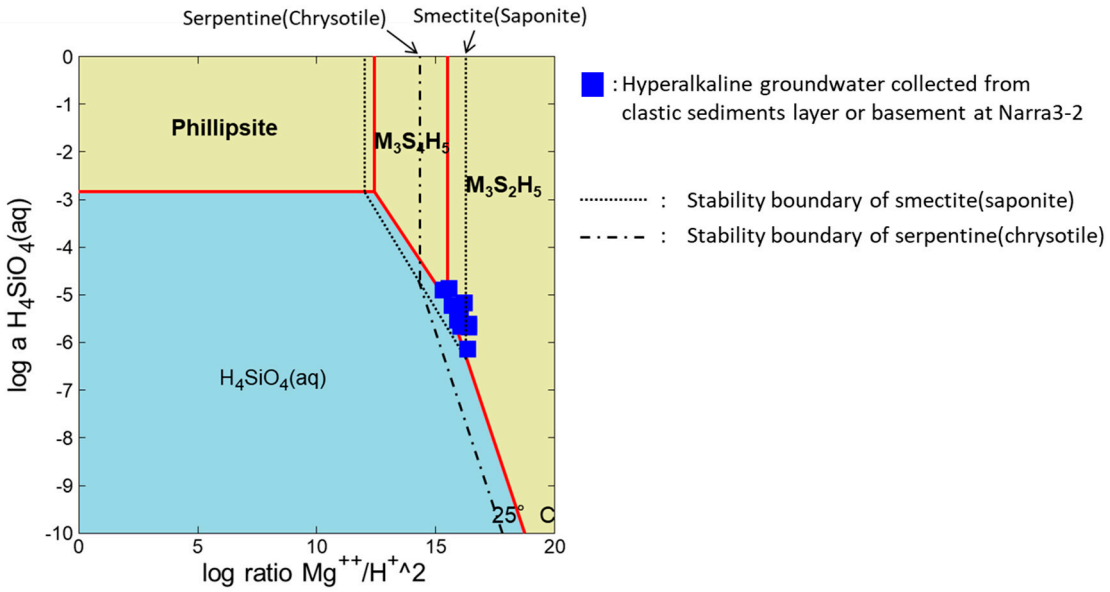

Figure 8. Phase diagram for Mg-Si-Al-Na system. Blue squares represent hyperalkaline groundwater collected from clastic sediments layer or basement at Narra3-2. Dotted lines show stability boundaries of smectite (saponite) and serpentine (chrysotile). ; $M_3S_4H_5$: M-S-H($3MgO{\cdot}4SiO_2{\cdot}5H_2O$); $M_3S_2H_5$: M-S-H($3MgO{\cdot}2SiO_2{\cdot}5H_2O$)

The smectite formed at matrix of clastic sediments from deeper parts shows the same occurrences with amorphous or poorly crystalline materials such as M-S-H from shallower parts. A previous study reported that a structure of M-S-H might be similar with 2:1 phyllosilicates with vacancies of Si in tetrahedral sites [16]. Because of structural and chemical similarities between M-S-H and smectite, there is a possibility that M-S-H was precipitated from hyperalkaline groundwater first by the interaction between clastic sediments and hyperalkaline groundwater, and alters to smectite. Although the relation with dissolved Fe^{2+} or Fe^{3+} concentration and formation of F-S-H has not been understood, F-S-H might be precipitated or coprecipitated with M-S-H, and form solid phase with Si, Fe and Mg.

Chemistry of hyperalkaline groundwater is governed by geochemical reactions of meteoric waters with Palawan ophiolite. Therefore, hyperalkaline groundwater have more likely been

Preprints (www.preprints.org) | NOT PEER-REVIEWED | Posted: 16 February 2018 doi:10.20944/preprints201802.0107.v1

Peer-reviewed version available at Minerals 2018, 8, 155; doi:10.3390/min8040155

flowing much longer than the deposition of clastic sediments at the site, and clastic sediments have more likely been interacting with hyperalkaline groundwater since clastic sediments have deposited at Narra3-2. ^{14}C dating of wooden branches in sediments collected from different depth at T5 shows burial age of wooden branches from deeper place is older than that from shallow place. This indicates clastic sediments at Narra3-2 might have deposited gradually. Therefore, estimated time-scale of the interaction between sediments and hyperalkaline groundwater is basically longer when sediments are present at deeper place. This is consistent that smectite was formed at matrix of clastic sediments from deeper parts (e.g. sample from DH4 at depth 6m) and amorphous or poorly crystalline material such as M-S-H and F-S-H was formed at matrix of clastic sediments from shallower parts (e.g. sample from DH4 at depth 3m).

These results suggest that smectite was produced under hyperalkaline conditions via amorphous or poorly crystalline material such as M-S-H and F-S-H by the interaction between clastic sediments and hyperalkaline groundwater. Because ^{14}C dating of wooden branches might indicate deposition age of wooden branches as well as the sediments, the age also indicates interaction time-scale between clastic sediments and hyperalkaline groundwater. Therefore, a certain amount of smectite might likely be produced under hyperalkaline conditions for thousands of years or more.

5.5. Implications from this study

Fe- or Mg-rich smectite have also been detected in Noachian-aged and early Hesperian-aged terrains on Mars [20,21]. A generally-accepted formation pathway of smectite is aqueous alteration of mafic rocks in surface or subsurface environments at neutral to alkaline pH [20,22]. Therefore, formation process of smectite in our studied area is analogue with generally-accepted pathway that might have been occurred on early Mars. This indicates that our suggested process of smectite formation under hyperalkaline conditions is not extraordinary process, and might have been occurred as well as on early Mars.

Many previous experimental works reported the formation of zeolite after alkaline alteration of bentonite [1–3]. On the other hand, natural analogue study at Zambales ophiolite reported the formation of smectite after alkaline alteration of bentonite [4]. Because smectite might play an important role for hydrologic barrier and nuclides isolation performance in the repository, it is important to understand factors determined secondary mineral species. Our study proposed that smectite were altered from amorphous or poorly crystalline material such as M-S-H and/or F-S-H under hyperalkaline conditions. Previous studies reported that a certain amount of Mg^{2+} and/or Fe^{2+} is necessary for the three-layer silicate minerals even during synthesize of Al^{3+}- or Fe^{3+}-rich smectite at low temperature [23,24]. From our study and that previous studies [23,24], key factor which decides smectite or zeolite as secondary minerals after alkaline alteration of bentonite might be whether nuclei of M-S-H and/or F-S-H will be formed or not.

Previous natural analogue study in Cyprus reported the naturally-occurring formation of Fe-bearing palygorskite as a result of bentonite alteration by alkaline fluids [8]. Because constituent elements of Fe-bearing palygorskite include Mg and Fe, a certain amount of Mg^{2+} (and Fe^{2+}) will be expected in the system. Factors that differed smectite or palygorskite as secondary minerals after alkaline alteration of bentonite are still unknown.

6. Conclusions

In present paper, Fe- and Mg-rich smectite in clastic sediments which are currently interacting with hyperalkaline groundwater was found at Narra in Palawan, Philippines. Hyperalkaline groundwater is likely caused by geochemical reactions of meteoric water with Palawan ophiolite. Fe- and Mg-rich smectite and amorphous or poorly crystalline material such as M-S-H and F-S-H show the same occurrences, and they were formed at matrix of clastic sediments as major infilling minerals at the site. From chemistry of hyperalkaline groundwater and occurrences, M-S-H might precipitate from hyperalkaline groundwater. The presence of authigenic tobermorite as infilling material also support that major infilling materials at matrix of clastic sediments formed by

Preprints (www.preprints.org) | NOT PEER-REVIEWED | Posted: 16 February 2018 doi:10.20944/preprints201802.0107.v1

Peer-reviewed version available at Minerals 2018, 8, 155; doi:10.3390/min8040155

interaction between the clastic sediments and hyperalkaline groundwater. Therefore, a certain amount of smectite might have been produced under hyperalkaline conditions, altered from amorphous or poorly crystalline material such as M-S-H and F-S-H.

Our suggested formation process of smectite under alkaline conditions is analogue with generally-accepted model of smectite formation that might have been occurred on early Mars. This indicates that our suggested formation process is not extraordinary process.

In the repository of radioactive wastes, alkaline alteration of bentonite is concerned. It might be crucial for safety assessment whether smectite will be formed or not as secondary minerals after alkaline alteration of bentonite. This is because smectite might play an important role for hydrologic barrier and nuclides isolation performance in the repository. Our study provides more understanding about secondary mineral formation after bentonite dissolution under hyperalkaline conditions in the repository. Key factor which decides smectite or zeolite as secondary minerals after alkaline alteration of bentonite might be whether nuclei of M-S-H and/or F-S-H will be formed or not. This might be decided by the presence of dissolved Mg^{2+} and Fe^{2+} in the system. Therefore, Mg^{2+} and Fe^{2+} should be examined carefully when we consider the interaction between bentonite and hyperalkaline fluids in the future works.

Acknowledgments: This research was initiated within a project of "natural analogue study" to develop geological disposal technologies in Japan, which was funded by the Ministry of Economy Trade and Industry (METI), Japan. The authors would like to thank to Mr. Yukinobu Kimura in Obayashi Corporation for fluids analyses, Dr. W. Russell Alexander in Bedrock Geosciences and Prof. Carlo Arcilla in University of the Philippines for valuable advices throughout this research and set up field survey, and Dr. Hisao Satoh in Mitsubishi Materials Corporation for EPMA analyses. The authors also thank to Mr. Masanobu Nishimura in Obayashi Corporation and Mr. Tatsuaki Nakazuka in Kiso-Jiban Consultants Corporation for field survey. Analyses of ^{14}C dating were performed under the Shared Use Program of JAEA Facilities [JAEA-AMS-TONO].

Author Contributions: M.S. is principal author conducting field survey, sampling, analyses, experiments, and writing this paper. T.S. is chief supervisors of M.S. in master course. T.S. designed this study. T.O. is also one of supervisors and conducted field survey and geochemical consideration. N.F. is principal manager of this project. M.Y. contributed to this study as geologist and petrologist.

Conflicts of Interest: The authors declare no conflict of interest.

References

1. Fernàndez, R.; Cuevas, J.; Sànchez, L.; Vigil de la Villa, R.; Santiago, L. Reactivity of the cement – bentonite interface with alkaline solutions using transport cells. *Appl. Geochemistry* **2006**, *21*, 977–992, doi:10.1016/j.apgeochem.2006.02.016.
2. Vigil de la Villa, R.; Cuevas, J.; Ramîrez, S.; Leguey, S. Zeolite formation during the alkaline reaction of bentonite. *Eur. J. Mineral.* **2001**, 635–644, doi:10.1127/0935-1221/2001/0013-0635.
3. Ruiz, R.; Blanc, C.; Pesquera, C.; Gonzilez, F.; Lpez, J. L.; Benito, I. Zeolitization of a bentonite and its application to the removal of ammonium ion from waste water. *Appl. Clay Sci.* **1997**, *12*, 73–83.
4. Fujii, N.; Yamakawa, M.; Shikazono, N.; Sato, T. Geochemical and Mineralogical Characterizations of Bentonite interacted with Alkaline Fluids generating in Zambales Ophiolite , Northwestern Luzons , Philippines. *Geol. Soc. Japan* **2014**, *120*, 361–375, doi:10.5575/geosoc.2014.0036.
5. Mitchell, A. H. G.; Hernandez, F.; Cruz, A. P. Dela Cenozoic evolution of the Philippine Archipelago. *J. Southeast Asian Earth Sci.* **1986**, *1*.
6. Aurelio, M. A.; Forbes, M. T.; Joy, K.; Taguibao, L.; Savella, R. B.; Bacud, J. A.; Franke, D.; Pubellier, M.; Savva, D.; Meresse, F.; Steuer, S.; Carranza, C. D. Middle to Late Cenozoic tectonic events in south and central Palawan (Philippines) and their implications to the evolution of the south- eastern margin of South China Sea: Evidence from onshore structural and offshore seismic data. *Mar. Pet. Geol.* **2014**, *58*, 658–673, doi:10.1016/j.marpetgeo.2013.12.002.

Preprints (www.preprints.org) | NOT PEER-REVIEWED | Posted: 16 February 2018 doi:10.20944/preprints201802.0107.v1

Peer-reviewed version available at Minerals 2018, 8, 155; doi:10.3390/min8040155

7. Nied, D.; Enemark-rasmussen, K.; Hopital, E. L.; Skibsted, J.; Lothenbach, B. Properties of magnesium silicate hydrates (M-S-H). *Cem. Concr. Res.* **2016**, *79*, 323–332, doi:10.1016/j.cemconres.2015.10.003.
8. Milodowski, A. E.; Norris, S.; Alexander, W. R. Minimal alteration of montmorillonite following long-term interaction with natural alkaline groundwater◎: Implications for geological disposal of radioactive waste. *Appl. Geochemistry* **2016**, *66*, 184–197, doi:10.1016/j.apgeochem.2015.12.016.
9. Anraku, S.; Matsubara, I.; Morimoto, K.; Sato, T. Geochemical Factors for Secondary Mineral Formation at Naturally-Occurring Hyperalkaline Spring in Oman Ophiolite. *J. Clay Sci. Soc. Japan* **2017**, 17–30.
10. Barnes, I.; Neil, J. R. O. The Relationship between Fluids in Some Fresh Alpine-Type Ultramafics and Possible Modern Serpentinization, Western United States. *Geol. Soc. Am. Bull.* **1969**, *80*, 1947–1960.
11. Bruni, J.; Canepa, M.; Chiodini, G.; Cioni, R.; Cipolli, F.; Longinelli, A.; Marini, L.; Ottonello, G.; Vetuschi, M. Irreversible water – rock mass transfer accompanying the generation of the neutral , Mg – HCO 3 and high-pH , Ca – OH spring waters of the Genova province , Italy. *Appl. Geochemistry* **2002**, *17*, 455–474.
12. Suzuki, S.; Sinn, E. 1.4 nm tobermorite-like calcium silicate hydrate prepared at room temperature from Si(OH)4 and CaCl2 solutions. *J. Mater. Sci. Lett.* **1993**, *12*, 542–544.
13. Hong, S.; Glasser, F. P. Alkali binding in cement pastes Part I . The C-S-H phase. *Cem. Concr. Res.* **2000**, *29*, 1893–1903.
14. Decarreau, A.; Colin, F.; Herbillon, A.; Manceau, A.; Nahon, D.; Paquet, H.; Trauth-badaud, D.; Trescases, J. J. DOMAIN SEGREGATION IN Ni-Fe-Mg-SMECTITES. *Clays Clay Miner.* **1987**, *35*, 1–10.
15. Gainey, S. R.; Hausrath, E. M.; Adcock, C. T.; Ehlmann, B. L.; Xiao, Y.; Bartlett, C. L.; Tschauner, O.; Hurowitz, J. A. Clay mineral formation under oxidized conditions and implications for paleoenvironments and organic preservation on Mars. *Nat. Commun.* **2017**, 1–7, doi:10.1038/s41467-017-01235-7.
16. Roosz, C.; Grangeon, S.; Blanc, P.; Montouillout, V.; Lothenbach, B.; Henocq, P.; Giffaut, E.; Vieillard, P.; Gaboreau, S. Crystal structure of magnesium silicate hydrates (M-S-H): The relation with 2◎: 1 Mg – Si phyllosilicates. *Cem. Concr. Res.* **2015**, *73*, 228–237, doi:10.1016/j.cemconres.2015.03.014.
17. Zhang, T.; Vandeperre, L. J.; Cheeseman, C. R. Formation of magnesium silicate hydrate (M-S-H) cement pastes using sodium hexametaphosphate. *Cem. Concr. Res.* **2014**, *65*, 8–14, doi:10.1016/j.cemconres.2014.07.001.
18. Decarreau, A.; Bonnin, D. SYNTHESIS AND CRYSTALLOGENESIS AT LOW TEMPERATURE OF FE (III) -SMECTITES BY EVOLUTION OF COPRECIPITATED GELS: EXPERIMENTS IN PARTIALLY REDUCING CONDITIONS. *Clay Miner.* **1986**, *21*, 861–877.
19. Decarreau, A.; Bonnin, D.; Badaut-trauth, D.; Couty, R.; Kaiser, P. SYNTHESIS AND CRYSTALLOGENESIS OF FERRIC SMECTITE BY EVOLUTION OF SI-FE COPRECIPITATES IN OXIDIZING CONDITIONS. *Clay Miner.* **1987**, *2*, 207–223.
20. Bishop, J. L.; Loizeau, D.; Mckeown, N. K.; Saper, L.; Dyar, M. D.; Des, D. J.; Parente, M.; Murchie, S. L. What the ancient phyllosilicates at Mawrth Vallis can tell us about possible habitability on early Mars. *Planet. Space Sci.* **2013**, *86*, 130–149, doi:10.1016/j.pss.2013.05.006.
21. Vaniman, D. T.; Bish, D. L.; Ming, D. W.; Bristow, T. F.; Morris, R. V; Blake, D. F.; Chipera, S. J.; Morrison, S. M.; Treiman, A. H.; Rampe, E. B.; Rice, M.; Achilles, C. N.; Grotzinger, J.; Mclennan, S. M.; Williams, J.; Iii, J. B.; Newsom, H.; Downs, R. T.; Maurice, S.; Sarrazin, P.; Yen, A. S.; Morookian, J. M.; Farmer, J. D.; Stack, K.; Milliken, R. E.; Ehlmann, B.; Sumner, D. Y.; Berger, G.; Crisp, J. A.; Hurowitz, J.

Preprints (www.preprints.org) | NOT PEER-REVIEWED | Posted: 16 February 2018 doi:10.20944/preprints201802.0107.v1

Peer-reviewed version available at Minerals 2018, 8, 155; doi:10.3390/min8040155

A.; Anderson, R.; Desmarais, D.; Stolper, E. M.; Edgett, K. S.; Gupta, S.; Spanovich, N.; Team, M. S. Mineralogy of a Mudstone at Yellowknife Bay , Gale Crater , Mars. *Sciencesxpress* **2013**, 1–15.

22. Chemtob, S. M.; Nickerson, R. D.; Morris, R. V; Agresti, D. G.; Catalano, J. G. Synthesis and structural characterization of Ferrous trioctahedral smectites: Implications for clay mineral genesis and detectability on Mars. *J. Geophys. Res. Planets* **2015**, *120*, 1119–1140, doi:10.1002/2014JE004763.Received.

23. Harder, H. THE ROLE OF MAGNESIUM IN THE FORMATION OF SMECTITE MINERALS. *Chem. Geol.* **1971**, *10*, 31–39.

24. Harder, H. NONTRONITE SYNTHESIS AT LOW TEMPERATURES. *Chem. Geol.* **1976**, *18*.